Electrophoresis of colloidal dispersions in the low-salt regime

Vladimir Lobaskin,[1, 2] Burkhard Dünweg,[1] Martin Medebach,[3] Thomas Palberg,[3] and Christian Holm[1, 4]

[1]*Max Planck Institute for Polymer Research, Ackermannweg 10, D-55128 Mainz, Germany*
[2]*Physik-Department, Technische Universität Munchen,*
James–Franck–Straße, D-85747 Garching, Germany
[3]*Institut für Physik, Johannes Gutenberg–Universität, Staudingerweg 7, D-55128 Mainz, Germany*
[4]*Frankfurt Institute for Advanced Studies (FIAS), J. W. Goethe–Universität,*
Max–von–Laue–Straße 1, D-60438 Frankfurt/Main, Germany
(Dated: Revised December 15, 2006)

We study the electrophoretic mobility of spherical charged colloids in a low-salt suspension as a function of the colloidal concentration. Using an effective particle charge and a reduced screening parameter, we map the data for systems with different particle charges and sizes, including numerical simulation data with full electrostatics and hydrodynamics and experimental data for latex dispersions, on a single master curve. We observe two different volume fraction-dependent regimes for the electrophoretic mobility that can be explained in terms of the static properties of the ionic double layer.

Many important properties of colloidal dispersions are directly or indirectly determined by the electric charge of the colloidal particles. Phase stability is provided by the repulsive interaction between like charges, while the details of the static and dynamic behavior are the result of the interplay between electrostatic interactions between macroions, counterions, and added salt ions, the dielectric response of the solvent, and the solvent hydrodynamics. Depending on whether the concentration of the background electrolyte (relative to that of the "native" counterions) is large or small, one must expect quite different behavior both with respect to statics and dynamics. The salt-dominated regime (high salt concentration) has been studied extensively both for static [1] and dynamic properties [2–5]. In this case, the large reservoir of salt ions results in a strong Debye screening of the electrostatic interactions between the macroions, such that the net charge density is essentially zero throughout the dispersion except for narrow ionic atmospheres around the colloids. An external electric field will therefore exert forces only within these layers, such that hydrodynamic interactions are also strongly screened in a system subjected to electrophoresis [6, 7]. Therefore, the problems both of ion cloud structure and of electrophoresis can be treated within a single-macroion framework [8], and the dependence of the electrophoretic mobility $\mu = v/E$ (v denoting the colloid drift velocity and E the driving electric field) on the macroion volume fraction Φ is weak.

Conversely, in the interesting regime of low salt concentration, where this screening is not present, the concentration dependence can be significant [9, 10]. From the theoretical point of view, this regime remains practically unexplored. The main goal of the present Letter is to find general relations between the electrophoretic mobility and other dispersion parameters in the counterion-dominated regime, based upon data from both computer simulations and experiments.

An important reference point in the case of low salt is the Hückel limit of electrokinetics. For an isolated colloidal sphere ($\Phi = 0$, salt concentration zero) with radius R and charge Ze (e denoting the elementary charge) in a solvent of viscosity η and dielectric constant ϵ, Stokes' law implies $\mu = Ze/(6\pi\eta R)$ (note that all counterions are infinitely far away). Furthermore, we introduce the Bjerrum length $l_B = e^2/(4\pi\epsilon k_B T)$, k_B and T denoting Boltzmann's constant and the temperature, respectively, as a characteristic length scale of electrostatic interactions. The reduced (dimensionless) mobility, defined as $\mu_{\rm red} = 6\pi\eta l_B \mu/e$, thus assumes the value $\mu_{\rm red} = Z l_B/R$ in the Hückel limit.

We are now interested in the case $\Phi > 0$ (but still salt-free). Some non-trivial statements about this regime can be made already in terms of dimensional analysis. $\mu_{\rm red}$, as a dimensionless quantity, can only depend on dimensionless combinations of the essential parameters of the system. These are: (i) $k_B T$ as a typical energy scale; (ii) l_B as the fundamental length scale of electrostatics (l_B may be viewed as re-parametrization of ϵ); (iii) the solvent viscosity η (or alternatively $\mu_0 = e/(6\pi\eta l_B)$) providing the fundamental time scale for viscous dissipation; (iv) the colloid radius R and (v) its valence Z; (vi) the colloid volume fraction Φ; and (vii) the radius a of the (monovalent) counterions (which we consider, due to Stokes' law, also as a measure of their mobility). Using the first three parameters as those which provide our fundamental unit system for energy, length, and time, we thus find $\mu_{\rm red} = \mu_{\rm red}(\Phi, Z, l_B/R, l_B/a)$.

We now introduce two further re-parametrizations. Firstly, we replace Z by $\tilde{Z} = Z l_B/R$, which would be equal to $\mu_{\rm red}$ in the $\Phi = 0$ limit. We expect that this change of variables results in a much weaker dependence on the last two parameters. This is obvious for $\Phi = 0$

where there is no dependence left; note also that l_B/a is typically of order unity for most systems. Secondly, in order to make contact with the standard parametrization used in the high-salt case [8, 11], we use the variable κR instead of Φ, where κ has the dimension of an inverse length, and $(\kappa R)^2 = 3\tilde{Z}\Phi$. Since the average counterion concentration is $n_i = Z/V$, where V is the average system volume per colloidal sphere, and $\Phi = 4\pi R^3/(3V)$, one sees that $\kappa^2 = 4\pi l_B n_i$, i. e. κ would have the interpretation of a Debye screening parameter if n_i were the salt concentration. We would like to stress, however, that these are mere re-parametrizations. This implies neither the interpretation of $\tilde{Z}$ as an electrostatic potential, nor of κ in terms of Debye screening. With these caveats in mind, we will call $\tilde{Z}$ the reduced charge, and κ the screening parameter [12]. From these considerations we expect that measurements for different systems should yield equal $\mu_{\rm red}$ values if the physical situations are identical in terms of the two parameters κR (or Φ), and $\tilde{Z}$. As we will show below, this is indeed the case.

As a final crucial step, we introduce *effective* values for the parameters Z and R (and correspondingly also Φ) and the effective reduced charge $\tilde{Z}_{\rm eff} = Z_{\rm eff} l_B/R_{\rm eff}$. While counterions far away from the colloid can be described reasonably well in terms of small Stokes spheres, co-moving with the surrounding hydrodynamic flow, this is much less obvious for those ions in the close vicinity of the colloid, which are tightly coupled to its motion. This is particularly true for highly charged systems. For this reason, we combine the central colloid with some of its counterions to an effective sphere with slightly increased R as well as decreased Z. $R_{\rm eff}$, the effective radius in the computer model, was defined as the minimum distance between the center of the colloid and the center of a counterion (see below). In the experiment, we set $R_{\rm eff} = R$ due to the smallness of the counterions. For determining $Z_{\rm eff}$ both in simulation and experiment, we applied the concept of charge renormalization [12–14]: After obtaining the full numerical solution of the Poisson-Boltzmann (PB) equation within the framework of the Wigner-Seitz cell model, this function was fitted to the solution of the corresponding linearized equation near the cell boundary [12]. Correspondingly, the screening parameter has to be calculated now with the effective counterion concentration, i. e. $n_i = Z_{\rm eff}/V$ for the salt-free system. The comparison between simulation and experiment is then done in terms of these effective parameters. The degree of charge renormalization is weak for small Z but is quite substantial for larger values (see below).

Our Molecular Dynamics (MD) computer model comprises small counterions, plus one large charged sphere, around which we wrap a network of small particles. All small particles are coupled dissipatively to a Lattice Boltzmann (LB) background [15, 16], which provides the hydrodynamic interactions. Thermal motion is taken into account via Langevin noise, and electrostatic interac-
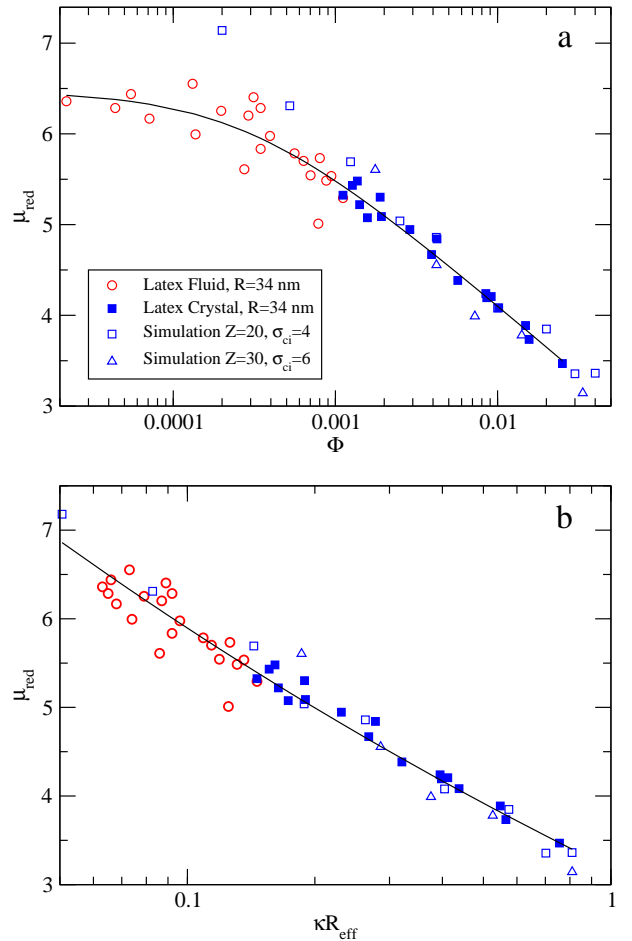

FIG. 1: Reduced electrophoretic mobility of a spherical particle vs. (a) particle volume fraction, and (b) reduced screening parameter, calculated from counterion and salt contributions (see text) for various systems with matching $\tilde{Z}$. The solid curves represent a fit to the experimental data.

tions are calculated via the Ewald summation technique. The system is simulated in a box with periodic boundary conditions, and thus corresponds to a well-defined finite value of Φ. In our unit system, we use $l_B = 1.3$, $R = 3$ or 5 and $Z = 20$, 30, or 60, while the small monovalent ions have diameter unity, which is also the LB lattice spacing. The closest colloid-ion separation was set to $\sigma_{ci} = R+1$, which was also taken as the effective macroion radius, $R_{\rm eff} = \sigma_{ci}$. For further details, see Refs. [17–19]. Applying an external electric field, and averaging the steady-state velocity of the colloid, we calculated μ. Some data points were compared with zero-field data obtained from Green-Kubo integration, confirming that the response is still in the linear regime. Due to the "screening" of hydrodynamic interactions (the total force on the system vanishes, due to charge neutrality, and thus does not generate a large-scale flow) [6, 7], we expect (and find, see below) only weak finite-size effects.

The experimental system comprises thoroughly deion-

ized aqueous suspensions of latex spheres (lab code PnBAPS68, kindly provided by BASF, Ludwigshafen, Germany) with diameter $2R = 68$nm, low polydispersity and high charge (bare charge $Z \approx 1500$; effective charge from conductivity $Z_\sigma^* = 450$ [20]). They show a low lying and narrow first order freezing transition at a particle number density of $n_F \approx (6.1 \pm 0.3)\mu m^{-3}$. Due to the small size optical investigations are possible without multiple scattering up to large n. Using Doppler velocimetry in the super-heterodyning mode [21] we studied the electrophoretic mobility in the range of $0.1\mu m^{-3} \leq n \leq 160\mu m^{-3}$, corresponding to volume fractions $\Phi = (4\pi/3)R^3 n$ of $5 \times 10^{-4} \leq \Phi \leq 2.5 \times 10^{-2}$ [22]. Consistent with data taken on other species and also at elevated salt concentrations [23], the mobility as shown in Fig. 1 exhibits a plateau at low Φ and descends fairly linearly in this semi-logarithmic plot at larger Φ. Charge renormalization [12] yields weakly varying values for Z_{eff}, resulting in $\tilde{Z}_{\text{eff}} \approx 8.5$ [24]. In the simulations we chose the parameter sets ($Z = 20, R = 3$) and ($Z = 30, R = 5$); these correspond to roughly the same value of $\tilde{Z}_{\text{eff}}$ in the dilute limit $\Phi \to 0$.

Comparing the experimental and simulated mobility data in Fig. 1a, where μ_{red} is shown as a function of Φ, one observes good agreement as long as Φ is not too small. However, simulation and experiment deviate in the regime of very low volume fractions. The reason is that for very small Φ the dissociation of water starts to play a role in the experiment — the size of the counterion cloud is no longer determined by the colloid-colloid distance, but rather by the background ionic concentration, so that it remains finite even at $\Phi = 0$. In principle, one must expect that the salt species will introduce yet another dimensionless parameter into the problem. However, we found that the effect of salt can be incorporated, within a reasonable approximation, by just adding the salt concentration to the counterion concentration, such that we obtain a new scaling variable κR_{eff} with $\kappa^2 = 4\pi l_B (n_i + n_{\text{salt}})$. The use of this procedure can be supported by the observation that the electrostatic potential in the regions centered between the colloids varies only weakly, such that a description in terms of a linearized PB equation is possible. In these regions, however, the local counterion concentration contributes to the screening parameter, too. Figure 1b shows that this strategy to include the effect of salt is indeed successful.

A qualitatively different behavior of μ_{red} is illustrated in Fig. 2, which shows the same simulation data as those of Fig. 1, augmented by an additional data set obtained at $Z = 60$. Upon stronger dilution μ_{red} for the system with $Z = 60$ increases sharply as $\Phi \to 0$ due to evaporation of the condensed ion layer, i. e. increase of Z_{eff}. In this regime, we find empirically $\mu_{\text{red}} \propto \Phi^{-1}$. Ultimately, at $\Phi = 0$ one would reach the "bare" limiting value $\mu_{\text{red}} = l_B Z/R = 26$. At the higher volume fractions $\Phi \geq 0.01$ charge renormalization yields $Z_{\text{eff}} < 30$,
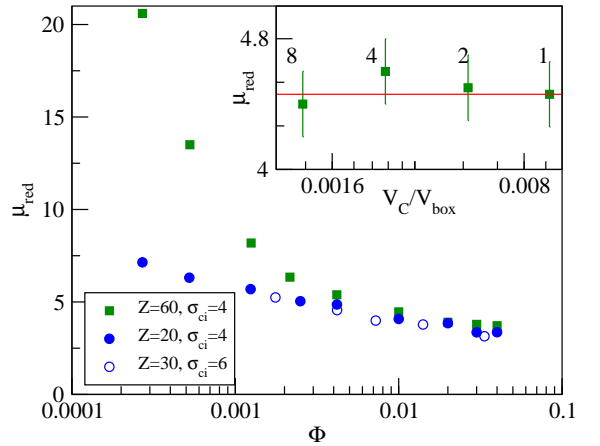

FIG. 2: Electrophoretic mobility of a spherical particle of the indicated charge and size as a function of the particle volume fraction in a salt–free system. The effective reduced charge $\tilde{Z}_{\text{eff}}$ is equal for the three systems at $\Phi \geq 0.01$, while it is growing in the system with $Z = 60$ upon stronger dilution. The inset shows the mobility of the particle of $Z = 60$ as a function of V_C/V_{box}, where V_C is the volume of one colloidal particle, and V_{box} is the system volume at constant Φ.
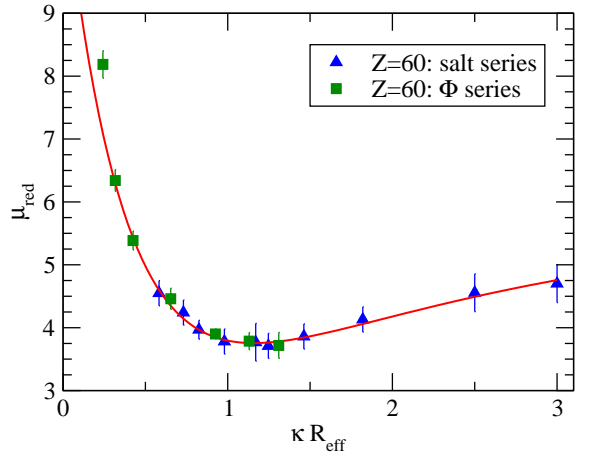

FIG. 3: Variation of the electrophoretic mobility of particles of charge $Z = 60$ in external field $Ee = 0.1$ versus the reduced screening parameter. The screening parameter was calculated from the concentration of the free ions at different colloid volume fractions and/or concentrations of added 1:1 salt. The curve is a guide to the eye.

giving rise to a reduced effective charge $\tilde{Z}_{\text{eff}} < 10$. In this high–concentration regime, Z_{eff} is fairly constant, and approaching that of the $Z = 20$, $Z = 30$ systems. Hence, the μ_{red} values are very similar, and again the mobility decreases logarithmically with Φ (as do the experimental data).

Although the behavior of μ_{red} is in general more complex, our parametrization still remains valid. In Fig. 3 we compare data obtained in a series of simulations at zero

salt concentration and increasing Φ to results of simulations at constant Φ but increasing amounts of added salt. The data coincide over a considerable region of κR_{eff}. The salt series curve continues with a slight increase, which is also a feature seen in the classical electrokinetic works [2, 3]. Yet, we note that the minimum on the electrophoretic mobility can be related to the general behavior of the ionic double layer for highly charged colloids [25]. The coincidence of the mobilities obtained for matching $\tilde{Z}_{\text{eff}}$ and κR_{eff} again supports our mapping postulate. Moreover, it clearly shows that the sort of ions present in the cloud is of minor importance for the mobility. The electrolyte effect, which leads to slowing down the particle drift, is produced in one case by solely counterions and in another case by both counterions and salt ions. In both cases it is only the *total* ion concentration that matters.

Finally, we briefly comment on finite-size effects. The same arguments that demonstrate hydrodynamic screening in systems with salt [6, 7] apply here, too. Therefore finite-size effects (as a result of image interactions) are expected to be weak, i. e. the single-colloid simulation should rather represent the many-colloid situation at the same volume fraction. We have explicitly tested this by increasing the number of particles at fixed Φ, which corresponds to a gradual transition from the symmetry of a cubic crystal to an isotropic liquid (corresponding to a bulk simulation [17]). The simulation results (see inset in Fig. 2) show that, within our numerical resolution, the mobility is not affected by the positions of the nearest neighbors. This is expected for a reasonably well–defined double layer, and corroborates the general effective single–particle picture, according to which the mobility is governed by the shear stresses within that layer. Quite analogously, one finds in the experiments that μ is remarkably smooth at the freezing transition (Fig. 1). Electrophoretic data on other particles as well as conductivity data show similar behavior [20, 24]. Moreover, our findings agree with recent numerical results for colloidal dispersions, employing the numerical solution of the Stokes and Poisson-Boltzmann equations [10, 26].

In summary, we have studied the electrophoretic mobility of colloidal particles in the counterion–dominated regime, which sets in at finite particle volume fractions and low electrolyte strengths. Based on the idea of static charge renormalization, we suggest a set of effective control parameters, the reduced effective particle charge $\tilde{Z}_{\text{eff}}$ and reduced screening constant κR_{eff}, controlling the static and dynamic properties of the system. Our model is supported by a successful matching of the LB/MD computer simulations of the primitive model electrolyte and Laser Doppler velocimetry measurements with similar $\tilde{Z}_{\text{eff}}$ and κR_{eff}, whose non-rescaled system parameters differ from each other by more than an order of magnitude. We believe that these results and observations constitute a first step towards understanding the physics of colloid electrophoresis in the low-salt limit.

[1] J. P. Hansen and H. Löwen, Ann. Rev. Phys. Chem. **51**, 209 (2000).
[2] P. H. Wiersema, A. L. Loeb, and J. T. G. Overbeek, J. Colloid Interface Sci. **22**, 70 (1966).
[3] R. O'Brien and L. White, J. Chem. Soc. Faraday Trans. **74**, 1607 (1978).
[4] M. Lozada-Cassou and E. Gonzáles-Tovar, J. Colloid Interface Sci. **239**, 285 (2001).
[5] F. Carrique, F. J. Arroyo, M. L. Jimenez, and A. V. Delgado, J. Phys. Chem. B **107**, 3199 (2003).
[6] D. Long and A. Ajdari, Eur. Phys. J. E **4**, 29 (2001).
[7] M. Tanaka and A. Y. Grosberg, J. Chem. Phys. **115**, 567 (2001).
[8] W. B. Russel, D. A. Saville, and W. R. Schowalter, *Colloidal Dispersions* (Cambridge University Press, Cambridge, 1989).
[9] H. Ohshima, J. Colloid Interface Sci. **188**, 481 (1997).
[10] K. Kim, Y. Nakayama, and R. Yamamoto, Phys. Rev. Lett. **96**, 208302 (2006).
[11] R. J. Hunter, *Zeta Potential in Colloid Science* (Academic Press, London, 1981).
[12] L. Belloni, Colloids and Surfaces A **140**, 227 (1998).
[13] S. Alexander, P. M. Chaikin, P. Grant, G. J. Morales, P. Pincus, and D. Hone, J. Chem. Phys. **80**, 5776 (1984).
[14] M. Aubouy, E. Trizac, and L. Bocquet, J. Phys. A Math. Gen. **36**, 5835 (2003).
[15] P. Ahlrichs and B. Dünweg, Int. J. Mod. Phys. C **9**, 1429 (1998).
[16] P. Ahlrichs and B. Dünweg, J. Chem. Phys. **111**, 8225 (1999).
[17] V. Lobaskin and P. Linse, J. Chem. Phys. **111**, 4300 (1999).
[18] V. Lobaskin and B. Dünweg, New J. Phys. **6**, 54 (2004).
[19] V. Lobaskin, B. Dünweg, and C. Holm, J. Phys. Condens. Matter **16**, S4063 (2004).
[20] P. Wette, H.-J. Schöpe, and T. Palberg, J. Chem Phys. **116**, 10981 (2002).
[21] M. Medebach and T. Palberg, J. Chem. Phys. **119**, 3360 (2003).
[22] M. Medebach and T. Palberg, J. Phys. Condens. Matter **16**, 5653 (2004).
[23] T. Palberg, M. Medebach, N. Garbow, M. Evers, A. B. Fontecha, and H. Reiber, J. Phys. Condens. Matter **16**, S4039 (2004).
[24] M. Medebach, R. Chulia-Jordan, H. Reiber, H.-J. Schöpe, R. Biehl, M. Evers, D. Hessinger, J. Olah, T. Palberg, E. Schönberger, et al., J. Chem. Phys. **123**, 104903 (2005).
[25] R. R. Netz and H. Orland, Eur. Phys. J. E **11**, 301 (2003).
[26] C.-P. Chiang, E. Lee, Y.-Y. He, and J.-P. Hsu, J. Phys. Chem. B **110**, 1490 (2006).